www.ietdl.org

Published in IET Power Electronics
Received on 25th April 2012
Revised on 9th September 2012
Accepted on 29th October 2012
doi: 10.1049/iet-pel.2012.0198

ISSN 1755-4535

Indirect output voltage regulation of DC–DC buck/boost converter operating in continuous and discontinuous conduction modes using adaptive backstepping approach

Mahdi Salimi[1], Jafar Soltani[2], Gholamreza Arab Markadeh[3], Navid Reza Abjadi[3]

[1]Department of Electrical Engineering, Science and Research Branch, Islamic Azad University, Tehran, Iran
[2]Department of Electrical Engineering, Khomeinishahr Branch, Islamic Azad University, Isfahan, Iran
(Emeritus Professor with the Faculty of Electrical Engineering, Isfahan University of Technology)
[3]Department of Engineering, Shahrekord University, Shahrekord, Iran
E-mail: m_salimi@srbiau.ac.ir

Abstract: In this study, an adaptive non-linear controller is designed for DC–DC buck/boost converter which is robust and stable against converter load changes, input voltage variations and parameter uncertainties. The proposed controller is developed based on input–output linearisation using an adaptive backstepping approach. The controller can be applied in both continuous and discontinuous conduction modes (CCM and DCM). Owing to non-minimum phase nature of buck/boost converter, the output voltage of this converter is indirectly controlled by tracking the inductor reference current. The inductor reference current is generated by a conventional PI controller. Using a MATLAB/Simulink toolbox and a stand-alone TMS320F2810 digital signal processor from Texas Instruments, some simulations and practical results are presented to verify the capability and effectiveness of the proposed control approach.

1 Introduction

DC–DC converters have recently aroused an increasing deal of interest both in power electronics and in automatic control. This is owing to their wide applicability domain that ranges from domestic equipment to advanced communication systems. They are also used in computers, industrial electronics, battery-operated portable equipment and uninterruptible power supply [1].

From an automatic control view-point, these closed-loop power converters are inherently non-linear systems. The major sources of non-linearity are switching non-linearity and interaction among the converter modules. For a non-linear converter with some uncertain parameters, assuming the load changes and its input voltage variations, small-signal analysis is not able to predict the converter steady-state and transient performances accurately [2].

To solve these problems, in the past decades some researchers have proposed different non-linear control methods such as sliding mode, fuzzy and adaptive control approaches [3–5]. Among these switching control methods, pulse width modulation (PWM) based on fast switching and duty ratio control may be the most extensively used. It is worthwhile to mention that the converter must be stable and robust against load disturbance, variations in input voltage and uncertainties that usually exist in converter parameters because of magnetic saturation and temperature variation.

It should be considered that, because of non-minimum phase nature of boost and buck/boost converters [6], it is difficult to regulate the converter output voltage directly.

In recent years, a few papers have been reported in continuous and discontinuous conduction modes (CCM and DCM) operations for indirect control of buck/boost converters [7–15].

In [7], an indirect controller is developed for isolated flyback DC–DC buck/boost converters with DCM operation, using peak-current current-mode control. In [7], the proposed control approach is based on small-signal modelling of the converter system. It is well known that such a linear analysis is not able to maintain converter stability and robustness in different operating-points.

In [8], a specific linearised technique around the equilibrium point is utilised to approximate whole non-linear system of the DC–DC boost converter. A simple analogue circuit is designed to implement the non-linear controller. One may note that by this method the stability of the whole actual system cannot be assured. In addition, DCM operation of the converter has not been investigated in [8].

In [9], an estimative current-mode control technique is reported for DC–DC converters and applied to a boost converter which operates in DCM. The principal idea of the proposed control scheme is to obtain samples of the required signals and estimate the required switch-on time using steady-state analysis of the converter. This controller has a fast dynamic response and can be implemented easily by digital processors. The major drawback of the current controller described in [9] is that for DCM operation, the converter duty cycle is estimated based on steady-state analysis. Also, the exact value of the inductor is needed to calculate the on-time of the converter switch. Furthermore, in [9] it is necessary to measure the input voltage of the converter that will increase converter implementation cost.

Sliding-mode (SM) control is well-known for good stability and regulation properties in a wide range of operating conditions. It is also deemed to be a better candidate than other non-linear controllers for its relative ease of implementation [16]. In particular, the fixed frequency PWM-based SM controllers, which amplify control signals obtained from SM control technique, are found to be suited for practical implementation in power converters [17].

A fixed frequency PWM-based SM controller is reported in [10] for buck, boost and buck/boost DC–DC converters, which is applicable to both CCM and DCM operations. The method described in [10] has been supported only by computer simulation results. Sliding-mode controller of [10] is in fact an SM following controller. Therefore it is not obtained based on a Lyapunov function; as a result it cannot be robust against load changes, input voltage variations and converter parameter uncertainties. In [10], it has been shown that when the load changes, a minimum steady-state error still exists in regulated output voltage. The main drawback of the SM method described in [10] is that it is applicable only for DCM operation and the converter duty cycle is obtained based on steady-state analysis of the converter. In addition, a high amount of SM chattering is seen in converter output voltage.

In [11], a digital SM current control of the DC–DC boost converter is reported which avoids continuous high frequency sampling of the controlled variables. In [11], a PI controller is used to regulate converter output voltage. The proposed control method in [11] is applicable only to CCM of operation and in addition, high SM chattering is seen in the converter output voltage waveform.

A two-loop microprocessor-based controller has been described in [12] for the DC–DC boost converter in CCM operation. The purpose of the inner loop is to control the inductor reference current based on variable band hysteresis current controller. The next loop provides a setpoint to the first control loop according to the output voltage error. Hysteresis current controller of [12] has some major disadvantages such as variable switching frequency, which makes converter implementation difficult. One may note that variable band hysteresis described in [12] is not able to solve this problem completely. Also, it cannot be applied in DCM operation.

A non-linear control strategy is described in [13] based on input–output feedback linearisation to solve the non-linearity and unstable zero-dynamics problems of the DC–DC boost converter operating in CCM. This non-linear controller requires an exact model of the converter. The controller reported in [13] is not robust against load changes, input voltage variations and parameter uncertainties. It can be said that the developed controller described in [13] is similar to a non-adaptive version of the backstepping controller proposed in [18]. Note that the DCM operation of the DC–DC boost converter has not been considered in [13, 18].

An adaptive backstepping control approach has been developed in [14] in order to control the DC–DC boost converter in CCM. In [14], it is assumed that the load resistance is uncertain and its value is estimated based on a suitable Lyapunov function. Also, a backstepping control of the DC–DC boost converter in the presence of coil magnetic saturation has been reported in [15].

In [14, 15], indirect output voltage regulation is accomplished through the regulation of inductor reference current, considering steady-state analysis of the converter. The methods described in [14, 15] have been supported only by computer simulation results. Also, these approaches are not robust and stable with reference to converter parameter uncertainties and input voltage variations. In addition, these proposed methods are only applicable for CCM operation of the converter. Moreover, the output voltage of the converter is controlled indirectly based on steady-state analysis with no closed-loop voltage control. For this reason, some steady-state error in converter output voltage is mandatory.

In [19], a multi-duty ratio modulation has been described for switching DC–DC buck converters. This technique achieves converter output voltage regulation by generating a control pulse train that is made up of control pulses with different duty ratios. This controller is based on steady-state analysis of the DC–DC buck converter in CCM and DCM operations. As a result it cannot guarantee controller stability and robustness against load disturbances, input voltage variations as well as with reference to converter parameter uncertainties. In [19], minimum and maximum duty ratios are assumed for converter CCM and DCM operations, which are obtained based on steady-state analysis of the converter. Note that during a load disturbance, the duty ratio of the converter is not predictable especially in DCM operation.

In [20], a fixed switching frequency robust controller has been developed for parallel DC–DC buck converters by combining the concepts of integral-variable structure and multiple-sliding surface control. The multi-surface SM controller of [20] is designed in two parts: the first controller is outside the boundary layer and the second controller is inside the boundary layer. For the first one, a smooth hyper surface is defined which is based on some assumptions that may not be valid in practice. The gains of each sliding surface are obtained by trial and error method. Although it has been said that the stability of the controller can be proved by Floquet theory or Lyapunov method, it has not been shown in the paper. In addition, in [20], although it is mentioned that the design of the SM controller is not based on the converter state averaged models, for designing the SM controller inside the boundary, the state-averaged model of the converter has been used. Moreover, in [20], the effectiveness of the proposed controller has been verified only by simulation results. Furthermore, the capability of the converter has not been investigated for DCM operation. Note that the proposed controller in [20] generates a high amount of SM chattering.

In [21], a conventional PI and an SM double-loop controller have been proposed for a buck/boost converter with wide range of load resistance and reference voltage. The controller of [21] has been verified only by computer simulation and is not valid for DCM operation of the converter.

Simulation results presented in [21], show that the buck/boost converter system is robust and stable against load disturbance and input voltage variations. In [21], the boundary width of the output voltage in sliding mode is found to be dependent on the circuit and control parameters. It means that for some uncertain parameters of the converter circuit, the SM boundary width becomes uncertain. As a result, the closed-loop system may not be stable. From the simulation results shown in [21], it can be seen that the converter dynamic response is not fast.

According to our search, recently no further published papers were found, which apply the adaptive non-linear control method to switch-mode DC–DC buck/boost converters in both DCM and CCM of operations.

In this paper, an adaptive non-linear current controller is developed for the DC–DC buck/boost converter which is robust and stable with respect to converter parameter uncertainties and variations in input voltage. Owing to the non-minimum phase nature of the buck/boost converter, the output voltage of this converter is indirectly controlled by tracking the inductor reference current. The inductor reference current is generated by a conventional PI controller. The proposed control technique is applicable to both CCM and DCM operations. In the DCM operating mode, the duration time in which the inductor current is zero, is assumed to be constant but has an unknown parameter similar to other converter parameters. The capability and effectiveness of the developed adaptive non-linear control approach is supported by simulation and experimental results.

2 Averaged state-space modelling of the DC–DC buck/boost converter

Assuming DCM operation of the DC–DC buck/boost converter, referring to Fig. 1, three different regions can be recognised. The state-space equations for each region can be derived as

$$X = [x_1 \ \ x_2]^{\mathrm{T}} = [i_L v_{\text{out}}]^{\mathrm{T}} \quad \text{state variables} \tag{1}$$

$$\dot{X} = A_1 X + B_1; \quad A_1 = \begin{bmatrix} -\frac{r_L}{L} & 0 \\ 0 & -\frac{1}{RC} \end{bmatrix}, \quad B_1 = \begin{bmatrix} \frac{v_{\text{in}}}{L} \\ 0 \end{bmatrix}$$

$$\text{when power switch is ON} \tag{2}$$

$$\dot{X} = A_2 X + B_2; \quad A_2 = \begin{bmatrix} -\frac{r_L}{L} & -\frac{1}{L} \\ \frac{1}{C} & -\frac{1}{RC} \end{bmatrix}, \quad B_2 = \begin{bmatrix} 0 \\ 0 \end{bmatrix}$$

$$\text{when power switch is OFF and } x_1 > 0 \tag{3}$$

$$\dot{X} = A_3 X + B_3; \quad A_3 = \begin{bmatrix} 0 & 0 \\ 0 & -\frac{1}{RC} \end{bmatrix}, \quad B_3 = \begin{bmatrix} 0 \\ 0 \end{bmatrix}$$

$$\text{when power switch is OFF and } x_1 = 0 \tag{4}$$

Considering averaged state-space modelling, the DC–DC buck/boost converter in DCM can be modelled as follows

$$\dot{x}_1 = \theta_1(1-u)x_2 + \theta_5 x_2 + \theta_4 u + \theta_7 x_1 \tag{5}$$

$$\dot{x}_2 = \theta_2(1-u)x_1 + \theta_6 x_1 + \theta_3 x_2 \tag{6}$$

where u (duty ratio) is the control input of the converter and

$$\theta_1 = -\frac{1}{L}; \quad \theta_2 = \frac{1}{C}; \quad \theta_3 = -\frac{1}{RC}; \quad \theta_4 = \frac{v_{\text{in}}}{L};$$
$$\theta_5 = \frac{\Delta}{L}; \quad \theta_6 = -\frac{\Delta}{C}; \quad \theta_7 = -\frac{r_L}{L}(1-\Delta) \tag{7}$$

Note that, if in (7) Δ is equated to zero, the converter model for CCM operation will be obtained.

3 Adaptive non-linear controller design

Block diagram of the developed two-loop controller is illustrated in Fig. 2. To eliminate the steady-state error of the system, a convectional PI controller is used to generate the inductor reference current.

Using the adaptive backstepping technique [22], an adaptive non-linear current controller is designed for the DC–DC buck/boost converter in the following steps.

Step 1: considering (5), the converter output current error can be defined by

$$\begin{aligned} z_1 &= x_1 - I_L \rightarrow \dot{z}_1 = \dot{x}_1 - I_L \\ &= \theta_1(1-u)x_2 + \theta_5 x_2 + \theta_4 u + \theta_7 x_1 - I_L \end{aligned} \tag{8}$$

where I_L is the inductor reference current. Considering the

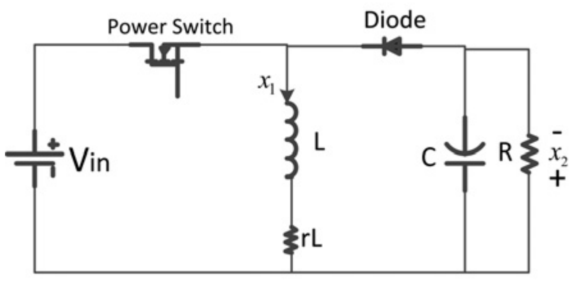

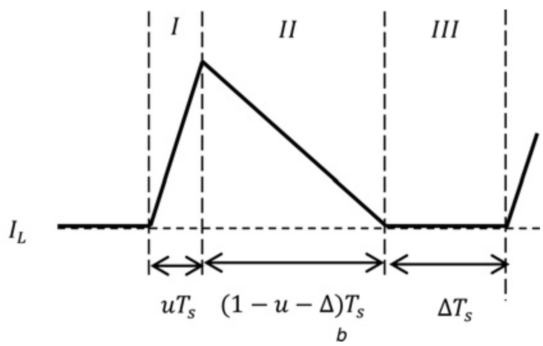

Fig. 1 *Inductor current of a DC–DC buck/boost converter operating in DCM*

a Power converter circuit
b Inductor current in different switching conditions

doi: 10.1049/iet-pel.2012.0198

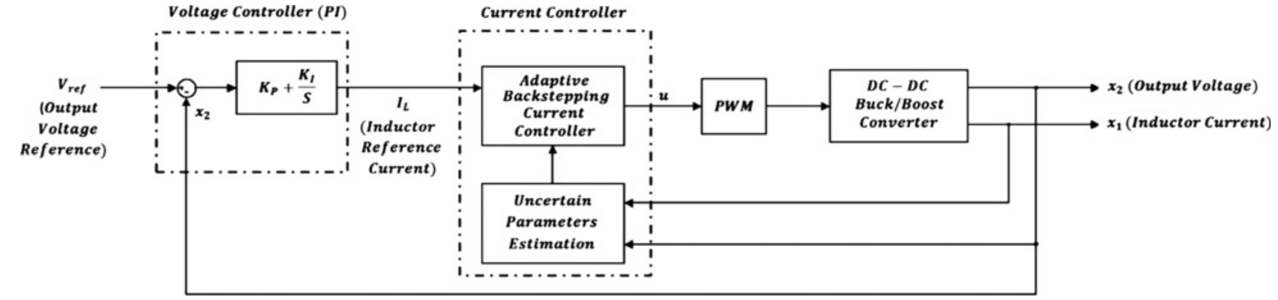

Fig. 2 *Designed two-loop controller*

unknown constant parameters for the converter, assuming estimation for converter parameters defined by $\hat{\theta}$, the matrix form of (8) can be written as

$$\dot{z}_1 = \hat{\boldsymbol{\theta}}^{\mathbf{T}} \boldsymbol{L}_1 - \dot{I}_L + \left(\boldsymbol{\theta} - \hat{\boldsymbol{\theta}}\right)^{\mathbf{T}} \boldsymbol{L}_1 \tag{9}$$

where

$$\hat{\boldsymbol{\theta}}^{\mathbf{T}} = \begin{bmatrix} \hat{\theta}_1 & \hat{\theta}_2 & \hat{\theta}_3 & \hat{\theta}_4 & \hat{\theta}_5 & \hat{\theta}_6 & \hat{\theta}_7 \end{bmatrix} \tag{10}$$

and

$$\boldsymbol{L}_1^{\mathbf{T}} = [(1-u)x_2 \quad 0 \quad 0 \quad u \quad x_2 \quad 0 \quad x_1] \tag{11}$$

Using a Lyapunov function as

$$V_1 = 0.5 z_1^2 + \left(\boldsymbol{\theta} - \hat{\boldsymbol{\theta}}\right)^{\mathbf{T}} \boldsymbol{\Gamma}^{-1} \left(\boldsymbol{\theta} - \hat{\boldsymbol{\theta}}\right) \tag{12}$$

where $\boldsymbol{\Gamma}$ is a positive-definite diagonal matrix whose elements $\gamma_{ii} (i = 1 \text{ to } 7)$ will be called system estimated parameter weights.

Derivative of V_1 with respect to time gives

$$\dot{V}_1 = z_1 \dot{z}_1 + \left(\boldsymbol{\theta} - \hat{\boldsymbol{\theta}}\right)^{\mathbf{T}} \boldsymbol{\Gamma}^{-1} \left(-\dot{\hat{\boldsymbol{\theta}}}\right) \tag{13}$$

Using (9), $\dot{V}_1$ is written as

$$\dot{V}_1 = z_1 \left(\hat{\boldsymbol{\theta}}^{\mathbf{T}} \boldsymbol{L}_1 - \dot{I}_L\right) + (\boldsymbol{\theta} - \hat{\boldsymbol{\theta}})^{\mathbf{T}} \boldsymbol{\Gamma}^{-1} \left(-\dot{\hat{\boldsymbol{\theta}}} + \boldsymbol{\Gamma} z_1 \boldsymbol{L}_1\right) \tag{14}$$

In (14), it is assumed that

$$\hat{\boldsymbol{\theta}}^{\mathbf{T}} \boldsymbol{L}_1 - \dot{I}_L = -c_1 z_1 \tag{15}$$

and

$$\left(-\dot{\hat{\boldsymbol{\theta}}} + \boldsymbol{\Gamma} z_1 \boldsymbol{L}_1\right) = 0 \tag{16}$$

then (14) becomes

$$\dot{V}_1 = -c_1 z_1^2 \le 0 \tag{17}$$

which is a negative semi-definite function and will result in asymptotically stable behaviour of the system. c_1 is a positive constant scalar.

Step 2: since $\hat{\boldsymbol{\theta}}^{\mathbf{T}} \boldsymbol{L}_1 - \dot{I}_L$ and $-c_1 z_1$ may not be equal, therefore a second error variable z_2 is defined as

$$z_2 = \hat{\boldsymbol{\theta}}^{\mathbf{T}} \boldsymbol{L}_1 - \dot{I}_L - (-c_1 z_1) \tag{18}$$

Using (10) and (11), z_2 is obtained as

$$z_2 = \hat{\theta}_1 (1-u) x_2 + \hat{\theta}_5 x_2 + \hat{\theta}_4 u + \hat{\theta}_7 x_1 - \dot{I}_L + c_1 z_1 \tag{19}$$

Combining (9) and (19) gives

$$\dot{z}_1 = -c_1 z_1 + z_2 + \left(\boldsymbol{\theta} - \hat{\boldsymbol{\theta}}\right)^{\mathbf{T}} \boldsymbol{L}_1 \tag{20}$$

From (19), the derivative of z_2 with respect to time in seconds is

$$\begin{aligned} \dot{z}_2 = {} & \dot{\hat{\theta}}_1 (1-u) x_2 + \hat{\theta}_1 (-\dot{u}) \dot{x}_2 + \hat{\theta}_1 (1-u) \dot{x}_2 + \dot{\hat{\theta}}_4 u + \hat{\theta}_4 \dot{u} \\ & + \dot{\hat{\theta}}_5 x_2 + \hat{\theta}_5 \dot{x}_2 + + \dot{\hat{\theta}}_7 x_1 + \hat{\theta}_7 \dot{x}_1 + c_1 \dot{z}_1 - \ddot{I}_L \end{aligned} \tag{21}$$

Using (5), (6) and (8), the general form of (21) can be shown by

$$\dot{z}_2 = A + \hat{\boldsymbol{\theta}}^{\mathbf{T}} \boldsymbol{L}_2 + \left(\boldsymbol{\theta} - \hat{\boldsymbol{\theta}}\right)^{\mathbf{T}} \boldsymbol{L}_2 \tag{22}$$

where

$$\begin{aligned} A = {} & \left[\dot{\hat{\theta}}_1 (1-u) x_2 + \dot{\hat{\theta}}_4 u + \dot{\hat{\theta}}_5 x_2 + \dot{\hat{\theta}}_7 x_1 - c_1 \ddot{I}_L - \ddot{I}_L\right] \\ & + \left(-\hat{\theta}_1 x_2 + \hat{\theta}_4\right)(\dot{u}) \end{aligned} \tag{23}$$

and

$$\boldsymbol{L}_2 = \begin{bmatrix} \left(c_1 + \hat{\theta}_7\right)(1-u) x_2 \\ \hat{\theta}_1 (1-u)^2 x_1 + \hat{\theta}_5 (1-u) x_1 \\ \hat{\theta}_1 (1-u) x_2 + \hat{\theta}_5 x_2 \\ \left(c_1 + \hat{\theta}_7\right)(u) \\ \left(c_1 + \hat{\theta}_7\right) x_2 \\ \hat{\theta}_1 (1-u) x_1 + \hat{\theta}_5 x_1 \\ \left(c_1 + \hat{\theta}_7\right) x_1 \end{bmatrix} \tag{24}$$

Introducing a second Lyapunov function as

$$V_2 = 0.5 z_1^2 + 0.5 z_2^2 + \left(\boldsymbol{\theta} - \hat{\boldsymbol{\theta}}\right)^{\mathbf{T}} \boldsymbol{\Gamma}^{-1} \left(\boldsymbol{\theta} - \hat{\boldsymbol{\theta}}\right) \tag{25}$$

From (25), one can obtain that

$$\dot{V}_2 = z_1 \dot{z}_1 + z_2 \dot{z}_2 + \left(\boldsymbol{\theta} - \hat{\boldsymbol{\theta}}\right)^{\mathbf{T}} \boldsymbol{\Gamma}^{-1} \left(-\dot{\hat{\boldsymbol{\theta}}}\right) \tag{26}$$

Considering (20) and (22), $\dot{V}_2$ can be changed to

$$\dot{V}_2 = -c_1 z_1^2 + z_1 z_2 + z_2\left(A + \hat{\boldsymbol{\theta}}^{\mathbf{T}}\boldsymbol{L}_2\right) + \left(\boldsymbol{\theta} - \hat{\boldsymbol{\theta}}\right)^{\mathbf{T}}\boldsymbol{\Gamma}^{-1}\left(-\dot{\hat{\boldsymbol{\theta}}} + \boldsymbol{\Gamma} z_1 \boldsymbol{L}_1 + \boldsymbol{\Gamma} z_2 \boldsymbol{L}_2\right) \quad (27)$$

If in (27), it is assumed that

$$A + \hat{\boldsymbol{\theta}}^{\mathbf{T}}\boldsymbol{L}_2 = -\boldsymbol{c}_2 z_2 \quad (28)$$

and

$$\left(-\dot{\hat{\boldsymbol{\theta}}} + \boldsymbol{\Gamma} z_1 \boldsymbol{L}_1 + \boldsymbol{\Gamma} z_2 \boldsymbol{L}_2\right) = 0 \quad (29)$$

then (27) is reduced to

$$\dot{V}_2 = -c_1 z_1^2 + z_1 z_2 - c_2 z_2^2 \quad (30)$$

where $c_2 > 0$ is a design constant. According to the Lyapunov stability theory, $\dot{V}_2$ must be a negative semi-definite function. Referring to (30), if $c_1 c_2 > (1/4)$, then $\dot{V}_2 \leq 0$. Hence, z_1 and z_2 are bounded. To indicate the convergence of z_1 and z_2 to zero, the following lemma is introduced.

Barbalat's lemma [23]: if a scalar function $V(x, t)$ satisfies the following conditions:

- $V(x, t)$ is lower bounded;
- $\dot{V}(x, t)$ is negative semi-definite;
- $\dot{V}(x, t)$ is uniformly continuous;

then $\dot{V}(x, t) \to 0$ as $t \to \infty$.

To use this lemma, let us check the uniform continuity of $\dot{V}_2$. The derivative e of $\dot{V}_2$ is

$$\ddot{V}_2 = -2c_1 z_1 \dot{z}_1 - 2c_2 z_2 \dot{z}_2 + z_1 \dot{z}_2 + z_2 \dot{z}_1 \quad (31)$$

Substituting for $\dot{z}_1$ and $\dot{z}_2$ from (20) and (21) in the above equation, since the errors of state variables (z_1, z_2) and parameters are bounded, $\ddot{V}_2$ becomes bounded. Hence, $\dot{V}_2$ is uniformly continuous. Application of Barbalat's lemma indicates that z_1 and z_2 converge to zero as $t \to \infty$ which will result in asymptotically stable behaviour of the system.

Combining (10), (11), (23), (24), (28) and (29), the adaptive non-linear current control effort (u) and estimation rules $\left(\hat{\theta}_i, i = 1 - 7\right)$ are obtained as

$$\dot{u} = \frac{-1}{-\hat{\theta}_1 x_2 + \hat{\theta}_4}\Big\{c_2 z_2 + \hat{\theta}_1(1-u)\big[(c_1 + \hat{\theta}_7)x_2 + \hat{\theta}_2(1-u)x_1 + \hat{\theta}_3 x_2 + \hat{\theta}_6 x_1\big]\hat{\theta}_2\hat{\theta}_5(1-u)x_1 + \hat{\theta}_3\hat{\theta}_5 x_2 + \hat{\theta}_6\hat{\theta}_5 x_1 + (c_1 + \hat{\theta}_7)\big[\hat{\theta}_4 u + \hat{\theta}_5 x_2 + \hat{\theta}_7 x_1\big] + \dot{\hat{\theta}}_1(1-u)x_2 + \dot{\hat{\theta}}_4 u + \dot{\hat{\theta}}_5 x_2 + \dot{\hat{\theta}}_7 x_1 - c_1\ddot{I}_L - \dddot{I}_L\Big\} \quad (32)$$

$$\dot{\hat{\theta}}_1 = \gamma_{11} x_2(1-u)\big[z_1 + (c_1 + \hat{\theta}_7)z_2\big] \quad (33)$$

$$\dot{\hat{\theta}}_2 = \gamma_{22} x_1(1-u)\big[(1-u)\hat{\theta}_1 + \hat{\theta}_5\big]z_2 \quad (34)$$

$$\dot{\hat{\theta}}_3 = \gamma_{33} x_2\big[(1-u)\hat{\theta}_1 + \hat{\theta}_5\big]z_2 \quad (35)$$

$$\dot{\hat{\theta}}_4 = \gamma_{44} u\big[z_1 + (c_1 + \hat{\theta}_7)z_2\big] \quad (36)$$

$$\dot{\hat{\theta}}_5 = \gamma_{55} x_2\big[z_1 + (c_1 + \hat{\theta}_7)z_2\big] \quad (37)$$

$$\dot{\hat{\theta}}_6 = \gamma_{66} x_1\big[(1-u)\hat{\theta}_1 + \hat{\theta}_5\big]z_2 \quad (38)$$

$$\dot{\hat{\theta}}_7 = \gamma_{77} x_1\big[z_1 + (c_1 + \hat{\theta}_7)z_2\big] \quad (39)$$

Equations (33)–(39) can be used for adaptive non-linear current control of DC–DC buck/Boost converter in CCM operation with $\Delta = 0$. For this mode of operation, the averaged state-space model of the converter is obtained as

$$\dot{x}_1 = \theta_1(1-u)x_2 + \theta_4 u + \theta_7 x_1 \quad \text{(state − space model in CCM)} \quad (40)$$

$$\dot{x}_2 = \theta_2(1-u)x_1 + \theta_3 x_2 \quad (41)$$

$$\theta_1 = -\frac{1}{L}; \quad \theta_2 = \frac{1}{C}; \quad \theta_3 = \frac{1}{RC}; \quad \theta_4 = \frac{v_{\text{in}}}{L}; \quad \theta_7 = -\frac{r_L}{L} \quad (42)$$

Using the same procedure as for the DCM operating condition, an adaptive backstepping current controller is designed which is only applicable to CCM operation of the converter. In this case, the control effort and parameter estimation rules are obtained as

$$\dot{u} = \frac{-1}{-\hat{\theta}_1 x_2 + \hat{\theta}_4}\Big\{c_2 z_2 + \hat{\theta}_1(1-u)\big[(c_1 + \hat{\theta}_7)x_2 + \hat{\theta}_2(1-u)x_1 + \hat{\theta}_3 x_2\big] + (c_1 + \hat{\theta}_7)\big[\hat{\theta}_4 u + \hat{\theta}_7 x_1\big] + \dot{\hat{\theta}}_1(1-u)x_2 + \dot{\hat{\theta}}_4 u + \dot{\hat{\theta}}_7 x_1 - c_1\ddot{I}_L - \dddot{I}_L\Big\} \quad (43)$$

$$\dot{\hat{\theta}}_1 = \gamma_{11} x_2(1-u)\big[z_1 + (c_1 + \hat{\theta}_7)z_2\big] \quad (44)$$

$$\dot{\hat{\theta}}_2 = \gamma_{22} x_1(1-u)\big[(1-u)\hat{\theta}_1\big]z_2 \quad (45)$$

$$\dot{\hat{\theta}}_3 = \gamma_{33} x_2\big[(1-u)\hat{\theta}_1\big]z_2 \quad (46)$$

$$\dot{\hat{\theta}}_4 = \gamma_{44} u\big[z_1 + (c_1 + \hat{\theta}_7)z_2\big] \quad (47)$$

$$\dot{\hat{\theta}}_7 = \gamma_{77} x_1\big[z_1 + (c_1 + \hat{\theta}_7)z_2\big] \quad (48)$$

$$z_2 = \hat{\theta}_1(1-u)x_2 + \hat{\theta}_4 u + \hat{\theta}_7 x_1 - \dot{I}_L + c_1 z_1 \quad (49)$$

4 Simulation and practical results

Considering a DC–DC buck/boost converter with electrical circuit shown in Fig. 1*a* and nominal specifications given in Table 1, some simulation and practical results are obtained for DCM and CCM operations of this converter.

A Texas digital signal processor (DSP) (TMS320F2810) has been used for practical implementation of the proposed control approach. An IL300 voltage isolated sensor and Hall Effect current sensor are used to measure converter output voltage and inductor current. Choosing a sampling frequency of 130 kHz and a converter switching frequency of 9.25 kHz, it is possible to sample 14 points in each switching period. The processor is fast enough to update the controller and estimation rules after each sampling. The

doi: 10.1049/iet-pel.2012.0198

Table 1 Nominal specifications of the DC–DC buck/boost converter

1	input voltage (v_{in}):	12 V
2	converter inductor (L):	550 μH
3	output capacitor (C):	330 μF
4	load resistance (R)	200 Ω
5	switching frequency (f_s):	9.25 kHz
6	inductor series resistance (r_L)	0.2 Ω
7	capacitor series resistance(r_C)	0.05 Ω

experimental setup and implemented power circuit are shown in Fig. 3. From this figure, one can see that step changes in parameters C and R are achieved by turning on and off the switches Q_2 and Q_3. Also switch Q_1 is used to change the input voltage. The converter state variables are measured and plotted by a 20 MHz PC-based digital oscilloscope.

Simulation and experimental results are obtained for some tests as described in the following:

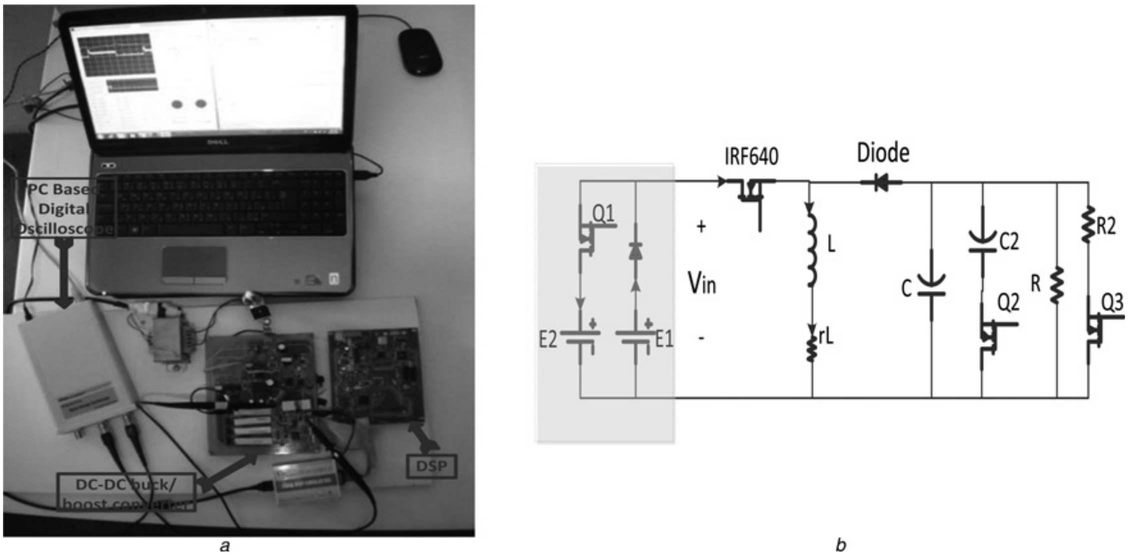

Fig. 3 *Experimental setup*

a Photograph of the real system
b Implemented power circuit

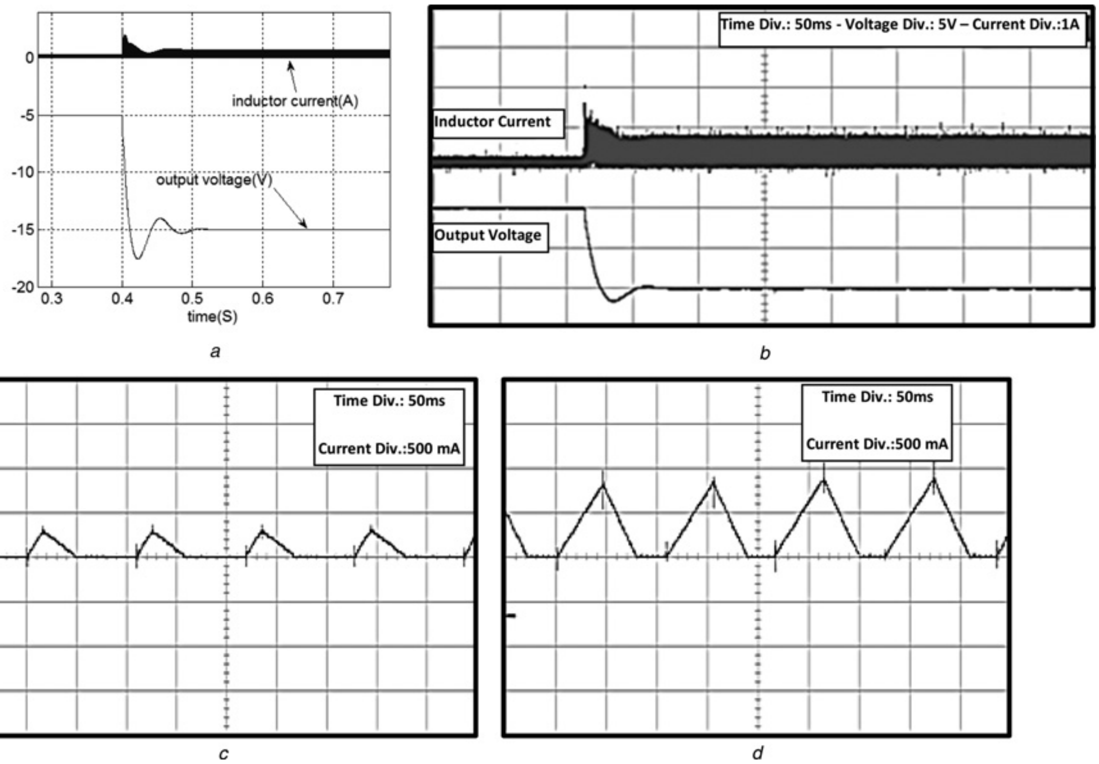

Fig. 4 *Step response of the proposed controller. At t=0.4 s, reference voltage is stepped up from −5 V to −15 V*

a Simulation
b Practical
c Inductor current ripple (practical) for $V_{ref} = -5$ V
d Inductor current ripple (practical) for $V_{ref} = -15$ V

Test 1: Considering the nominal values of the power circuit given in Table 1, the converter output reference voltage is stepped up from $V_{ref} = 5$ V to $V_{ref} = 15$ V at $t = 0.4$ s. For this condition simulation and practical results obtained are demonstrated in Fig. 4.

4.1 Buck operation

Test 2: Assume that the converter operates in a steady-state condition with $R = 100\ \Omega$ and $C = 660\ \mu$F and $V_{ref} = -5$ V. Considering a step change in load resistance and output capacitor to $R = 200\ \Omega$ and $C = 330\ \mu$F at $t = 0.4$ s and then back to primary values at $t = 0.6$ s, simulation and experimental results obtained for this condition are shown in Figs. 5*a* and *b*.

Test 3: Assuming an output reference voltage of $V_{ref} = -5$ V, simulation and experimental results of the DC–DC buck/boost converter to step changes of input voltage are shown in Fig. 6. In this test, at $t = 0.4$ s the input voltage is stepped up from +12 V to +17.

Test 4: Considering a steady-state DCM operation of the converter with $V_{ref} = -5$ V, $R = 200\ \Omega$, $V_{in} = 12$ V and $C = 330\ \mu$F; these values are stepped up to $R = 100\ \Omega$, $V_{in} = 17$ V and $C = 660\ \mu$F at t = 0.4 s. Simulation and experimental results obtained for this test are shown in Fig. 7.

4.2 Boost operation

Some tests are repeated for boost operation of the converter. In these tests, the converter output voltage reference is chosen to be $V_{ref} = -18$ V.

Test 5: Assume that the converter operates in steady state with $R = 100\ \Omega$. Considering a step change in load resistance to $R = 200\ \Omega$ at $t = 0.2$ s and then back to primary values at $t = 0.4$ s, simulation and experimental results obtained for this test are shown in Fig. 8. Under these conditions, the converter operates in DCM.

Test 6: Considering a steady-state DCM operation of the converter that is achieved by $R = 200\ \Omega$, $V_{in} = 27$ V and $C = 330\ \mu$F ; these values are stepped up to $R = 100\ \Omega$, $V_{in} = 17$ V and $C = 660\ \mu$F at $t = 0.3$ s and then back to primary values at $t = 0.65$ s. Simulation and experimental results obtained for this test are shown in Fig. 9.

4.3 Transition between DCM and CCM operations

Test 7: In this test, load resistance is stepped down from $R = 200\ \Omega$ to $R = 8.5\ \Omega$ at $t = 1.5$ s with $V_{ref} = -5$ V. Under these conditions, the operating mode of the converter is changed to CCM. Simulation and experimental results obtained for this test are shown in Fig. 10.

Note that simulation and practical results shown in Figs. 4–9 (DCM operation) are obtained for $c_1 = 25 \times 10^4$, $c_2 = 15 \times 10^3$, $K_P = 0.09$, $K_I = 20$ and $\gamma_{ii} = 1 \times 10^{-5}$ (for $i = 1$ to 7). In Fig. 10, $c_2 = 2 \times 10^3$ is selected to get CCM operation. These values are obtained by trial and error method based on achieving a reasonable system dynamic response.

From the simulation and experimental results presented in this paper, it seems that the dynamic response of the buck/boost converter is not quick enough. The reason for that could be because of assuming that all circuit parameters are uncertain. Such an assumption could cause a low convergence rate in estimating the circuit parameters, which could result in decreasing the rate of converter dynamic response.

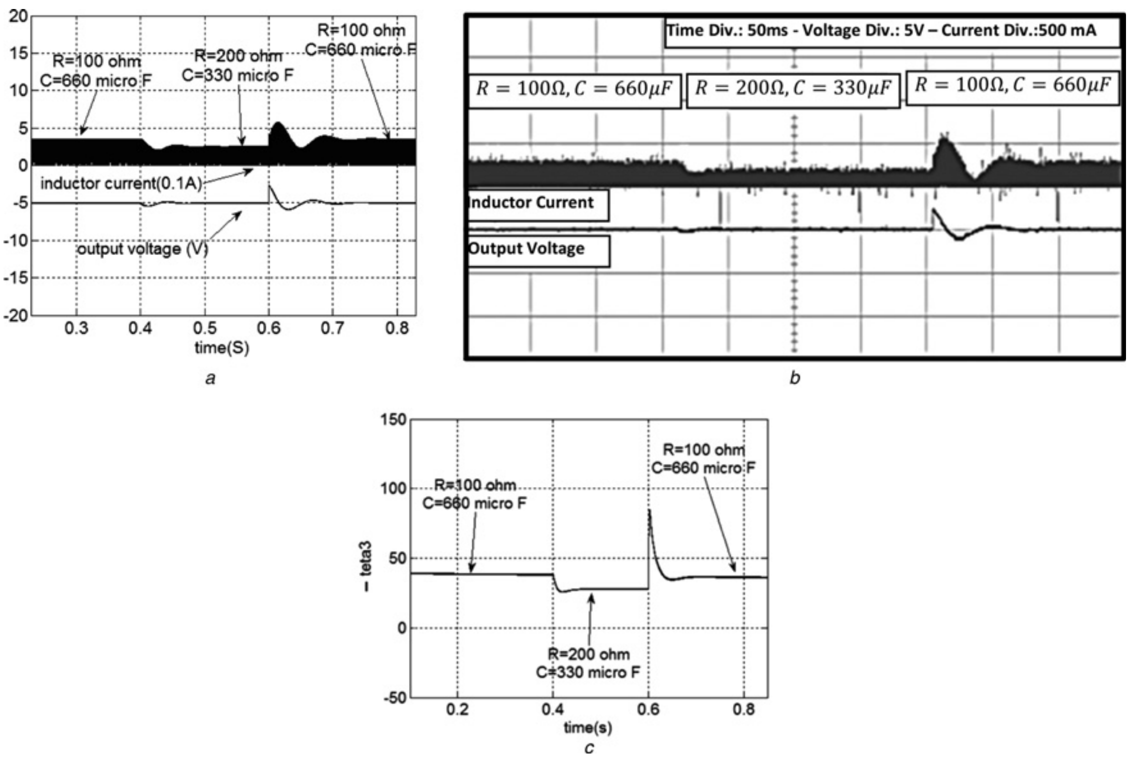

Fig. 5 *Response of the controller to step changes of R and C in DCM*

a Simulation
b Practical
c Estimated value of $-\theta_3$

doi: 10.1049/iet-pel.2012.0198

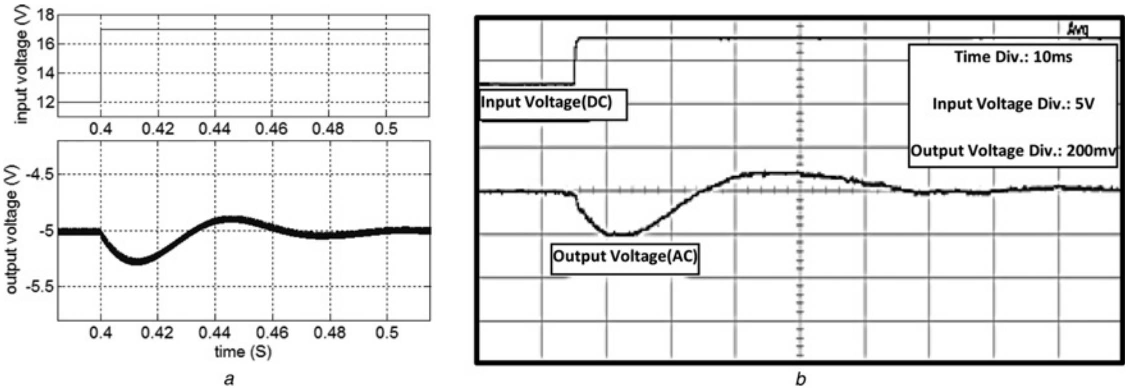

Fig. 6 *Response of the controller to step changes of input voltage in DCM*

a Simulation
b Practical

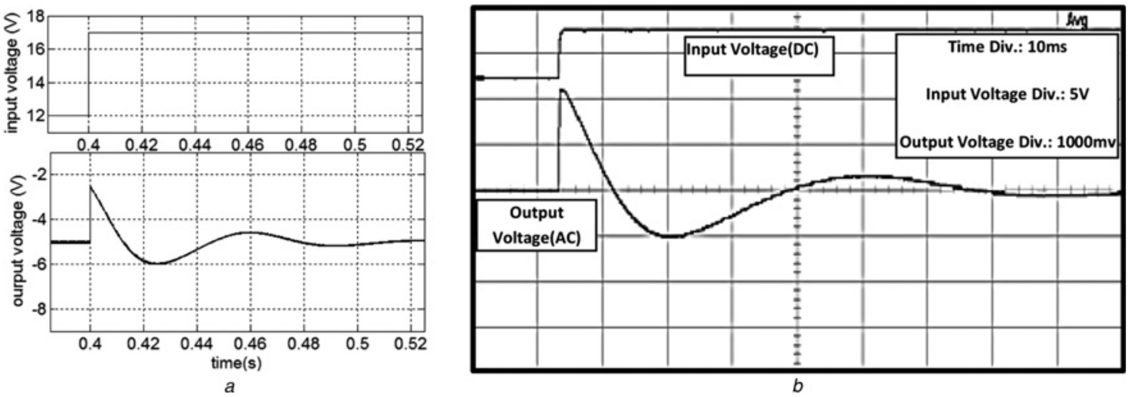

Fig. 7 *Simulation and experimental response of the proposed controller to simultaneous variations in input voltage, load resistance and output capacitor*

a Simulation
b Practical

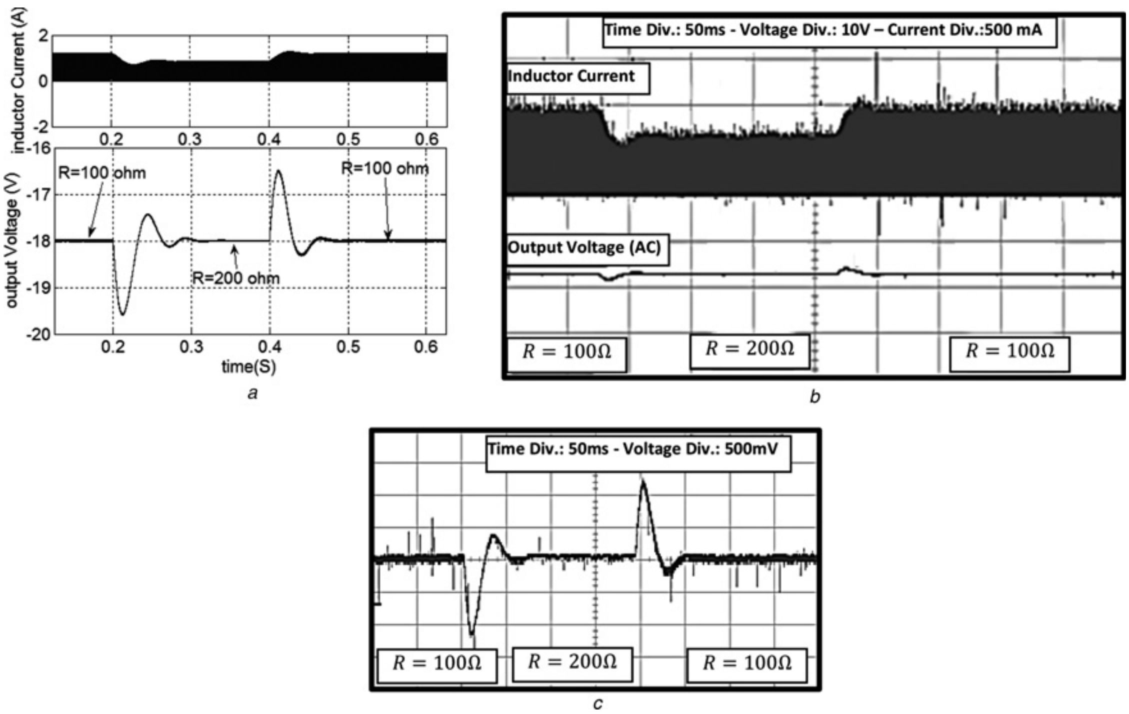

Fig. 8 *Response of the controller to step changes of R in DCM*

a Simulation
b Practical
c Output voltage in test 5 in more detail

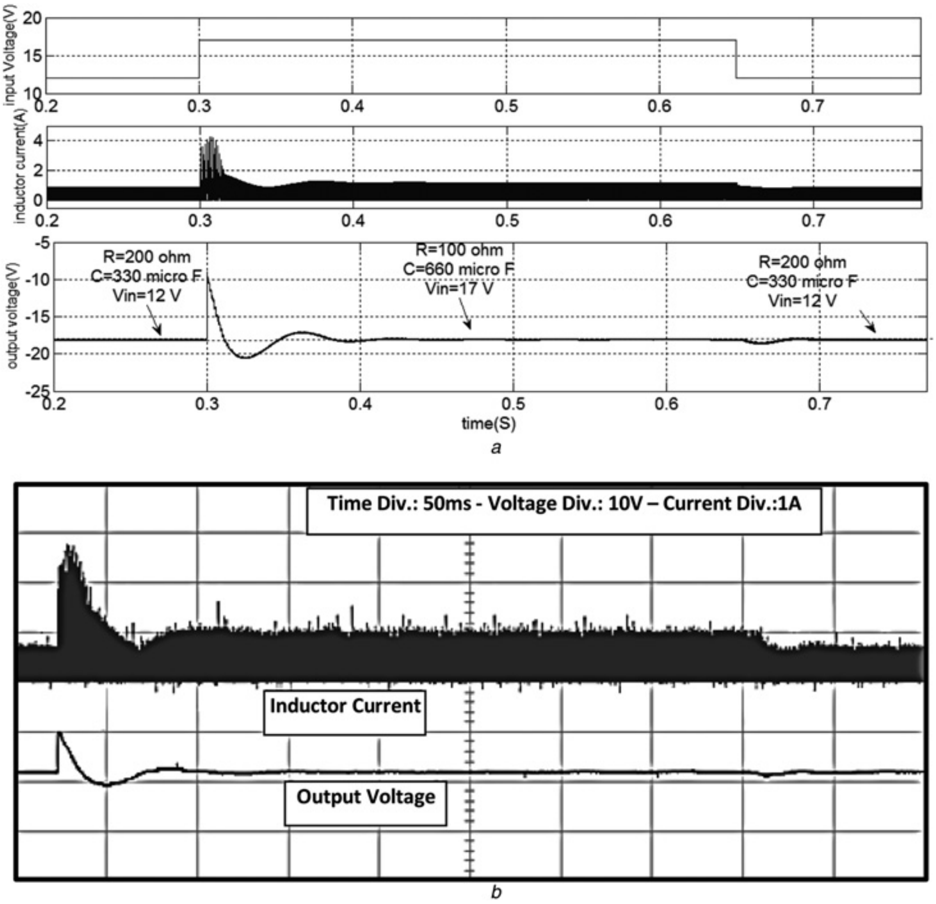

Fig. 9 *Simulation and experimental response of the proposed controller to simultaneous variations in input voltage, load resistance and output capacitor*

a Simulation
b Practical

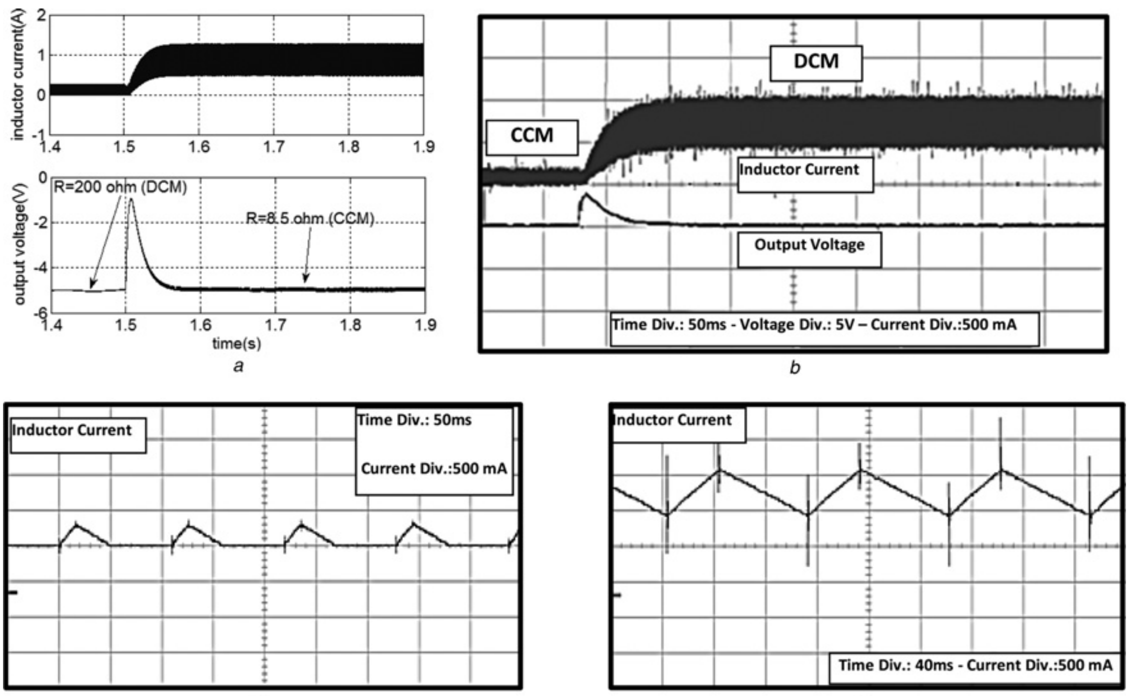

Fig. 10 *Response of the proposed controller during transition between DCM and CCM operations*

a Simulation
b Practical
c Inductor current ripple in DCM (practical)
d Inductor current ripple in CCM (practical)

IET Power Electron., 2013, Vol. 6, Iss. 4, pp. 732–741
doi: 10.1049/iet-pel.2012.0198

5 Conclusion

In this paper, the CCM and DCM operations of a DC–DC buck/boost converter have been investigated. An adaptive non-linear current controller has been developed based on input–output feedback linearisation using an adaptive backstepping control approach. Owing to non-minimum phase nature of the buck/boost converter, the output voltage of this converter is indirectly controlled by tracking inductor reference current. The inductor reference current is generated on-line by a conventional PI controller. Using a stand-alone TMS320F2810 DSP from Texas instruments, the effectiveness and capability of the proposed control approach has been supported by simulation and experimental results. Simulation and experimental results have been obtained for some tests. These results are corresponding to the converter CCM and DCM operations. These results confirm that the proposed controller is stable and robust with reference to converter uncertainty parameters, load disturbances and input voltage variations. In this control approach there is no need to know the operation mode of the converter.

6 References

1 Mohan, N., Undeland, T.M., Robbins, W.P.: 'Power electronics: converters, applications and design' (John Willey and Sons, Inc., 2004, 3rd edn.)

2 He, Y., Luo, F.L.: 'Sliding-mode control for DC–DC converters with constant switching frequency', *IEE Proc. Control Theory Appl.,* 2006, **153**, (1), pp. 37–45

3 Escobar, G., Ortega, R., Sira-Ramirez, H., Vilain, J.-P., Zein, I.: 'An experimental comparison of several nonlinear controllers for power converters', *IEEE Control Syst.*, 1999, **19**, (1), pp. 66–82

4 Mattavelli, P., Rossetto, L., Spiazzi, G., Tenti, P.: 'General-purpose fuzzy controller for DC-DC converters', *IEEE Trans. Power Electron.*, 1997, **12**, (1), pp. 79–86

5 Fadil, H., Giri, F.: 'Robust nonlinear adaptive control of multiphase synchronous buck power converters' control engineering practice (Elsevier, 2009), pp. 1245–1254

6 Fadil, H.E., Giri, F., Haloua, M., Ouadi, H., Chaoui, F.: 'Nonlinear and adaptive control of buck-boost power converters'. LAPISMRA 2002, 1996, vol. 11, pp. 578–584

7 Wu, K.C.: 'A comprehensive analysis of current-mode control for DCM buck-boost converters', *IEEE Trans. Ind. Electron.*, 2004, **51**, (3), pp. 733–735

8 Chan, C.-Y.: 'A nonlinear control for DC–DC power converters', *IEEE Trans. Power Electron*., 2007, **22**, (1), pp. 216–222

9 Ferdowsi, M., Emadi, A.: 'Estimative current mode control technique for DC–DC converters operating in discontinuous conduction mode', *IEEE Power Electron. Lett*., 2004, **2**, (1), pp. 20–23

10 Tan, S.-C., Lai, Y.M., Tse, C.K., Martinez-Salamero, L.: 'Special family of PWM-based sliding-mode voltage controllers for basic DC–DC converters in discontinuous conduction mode', *IET Electr. Power Appl.*, 2007, **1**, (1), pp. 64–74

11 Vidal-Idiarte, E., Carrejo, C.E., Calvente, J., Martínez-Salamero, L.: 'Two-loop digital sliding mode control of DC–DC power converters based on predictive interpolation', *IEEE Trans. Ind. Electron*., 2011, **58**, (6), pp. 2491–2501

12 De Keyser, R., Bonilla, J., Ionescu, C.: 'A comparative study of several control techniques applied to a boost converter'. IEEE Tenth Int. Conf. on Optimization of Electrical and Electronic Equipment OPTIM, Brasov Romania, 2006

13 Liu, J., Ming, W., Gao, F.: 'A new control strategy for improving performance of boost DC/DC converter based on input–output feedback linearization'. Proc. Eighth World Congress on Intelligent Control and Automation, Jinan, China, 6–9 July 2010

14 Fadil, H.E.L., Giri, F.: 'Backstepping based control of PWM DC-DC boost power converters', *Int. J. Power Eng.*, 2007, **1**, (5), pp. 479–485

15 Fadil, H.E.l., Giri, F., ElMagueri, O., Chaoui, F.Z.: 'Control of DC–DC power converters in the presence of coil magnetic saturation', *Control Eng. Pract., Elsevier J.*, 2009, **17**, pp. 849–862

16 Tan, S.-C., Lai, Y.M., Cheung, M.K.H., Tse, C.K.: 'On the practical design of a sliding mode voltage controlled buck converter', *IEEE Trans. Power Electron.,*, 2005, **20**, (2), pp. 425–437

17 Tan, S.-C., Lai, Y.M., Tse, C.K., Martinez-Salamero, L., Wu, C.-K.: 'A fast-response sliding-mode controller for boost-type converters with a wide range of operating conditions', *IEEE Trans. Ind. Electron.*, 2007, **54**, (6), pp. 3276–3286

18 Alvarez-Ramirez, J., Espinosa-Perez, G., Noriega-Pineda, D.: 'Current-mode control of DC–DC power converters: a backstepping approach'. Proc. IEEE Int. Conf. on Control Applications, 2001 (CCA '01), 2001, pp. 190–195

19 Qin, M., Xu, J.: 'Multi-duty ratio modulation technique for switching DC–DC converters operating in discontinuous conduction mode', *IEEE Trans. Ind. Electron.*, 2010, **57**, (10), pp. 3497–3507

20 Mazumder, S.K., Nayfeh, A.H., Borojević, D.: 'Robust control of parallel DC–DC buck converters by combining integral-variable-structure and multiple-sliding-surface control schemes', *IEEE Trans. Power Electron.*, 2002, **17**, (3), pp. 428–437

21 Chen, Z.: 'Double loop control of buck-boost converters for wide range of load resistance and reference voltage', *IET Control Theory Appl.*, 2012, **6**, (7), pp. 900–910

22 Rios-Bolivar, M., Sira-Ramirez, H., Zinober, A.S.I.: 'Output tracking control via adaptive input–output linearization: a backstepping approach'. Proc. 34th IEEE Conf. on Decision and Control, 13–15 December 1995, vol. 2, pp. 1579–1584

23 Slotine, J.J.E., Li, W.: 'Applied nonlinear control' (Prentice-Hall Press, 1991)

doi: 10.1049/iet-pel.2012.0198